STIMULUS REPORT

blood advances

High mitochondrial mass is associated with reconstitution capacity and quiescence of hematopoietic stem cells

Yuji Takihara,[1] Ayako Nakamura-Ishizu,[1,2] Darren Qiancheng Tan,[1] Masahiro Fukuda,[2,3] Takayoshi Matsumura,[1] Mitsuhiro Endoh,[1,4] Yuichiro Arima,[2,5] Desmond Wai Loon Chin,[6] Terumasa Umemoto,[2] Michihiro Hashimoto,[2] Hidenobu Mizuno,[2] and Toshio Suda[1,2]

[1]Cancer Science Institute of Singapore, National University of Singapore, Singapore; [2]International Research Center for Medical Sciences, Kumamoto University, Kumamoto, Japan; [3]Program in Neuroscience and Behavioral Disorders, Duke-NUS Medical School, Singapore; [4]Department of Pluripotent Stem Cell Biology, Institute of Molecular Embryology and Genetics, and [5]Department of Cardiovascular Medicine, Graduate School of Medical Sciences, Kumamoto University, Kumamoto, Japan; and [6]Genome Institute of Singapore, Singapore

Key Points

- HSCs can be separated based on high or low mitochondrial mass.
- Higher mitochondrial mass is associated with quiescence and greater reconstitution capacity of HSCs.

Introduction

Hematopoietic stem cells (HSCs) are capable of self-renewal and multilineage differentiation.[1,2] HSCs prefer glycolysis over mitochondrial oxidative phosphorylation for energy production.[3-5] This metabolic preference allows HSCs to limit reactive oxygen species (ROS) production and maintain HSC potential.[6,7] Although the function of mitochondria in HSCs is not fully understood, recent reports have suggested that they play important roles other than adenosine triphosphate production.[8,9] Contrary to the requirement to maintain low ROS levels, HSCs have recently been reported to exhibit higher mitochondrial mass (a major source of ROS) compared with more differentiated cells ($Lin^-Sca\text{-}1^-c\text{-}Kit^+$ cells),[10] which seemingly contradicts previous views that HSCs exhibit a low mitochondrial profile. However, whether mitochondrial mass varies among HSCs and is associated with cell cycle state and HSC function are largely unknown.

Here, we show, using superresolution imaging of HSCs from mito-Dendra2 (PhAM) mice[11] and droplet digital polymerase chain reaction (ddPCR), that mitochondrial mass varies within the HSC population. mito-Dendra2 fluorescence intensity in HSCs positively correlates with the expression of endothelial protein C receptor (EPCR).[12,13] Functionally, we show that HSCs with higher mitochondrial mass are more quiescent and have greater reconstitution capacity. Overall, this study clarifies the association between mitochondrial mass and HSC function and demonstrates that quiescent and potent HSCs are highly enriched within the mito-Dendra2^{hi} HSC fraction.

Methods

All experiments were performed according to protocols approved by the National University of Singapore Institution of Animal Care and Use Committee, and the Office of Safety, Health, and Environment. Detailed descriptions for all methods are described in the supplemental Methods.

Results and discussion

To address whether mitochondrial mass varies among HSCs, we first measured the fluorescence intensity of bone marrow (BM) HSCs ($CD150^+CD48^-$ $Lin^-Sca\text{-}1^+c\text{-}Kit^+$ [SLAM LSK] cells)[14] obtained from mito-Dendra2 mice, which express Dendra2 specifically in mitochondria[11] (Figure 1A; supplemental Figure 1A). Because mito-Dendra2 fluorescence intensity varied among HSCs, we analyzed mito-Dendra2^{lo} and mito-Dendra2^{hi} HSCs, defined as HSCs with the bottom 10% and top 10% of mito-Dendra2 fluorescence intensity, respectively (Figure 1A). We quantitated the mitochondrial mass of mito-Dendra2^{lo} and mito-Dendra2^{hi} HSCs using superresolution imaging of mitochondria with z-stacks.[15] In 3-dimensional imaging, optical aberrations due to refractive index mismatch between oil and mounting medium and imperfect spherical aberration correction lead to point spread function (PSF) enlargement (Figure 1B, left panel). Thus, we corrected PSF enlargement using images of fluorescent microspheres (Figure 1B, right panel) and quantified 3-dimensional mitochondrial mass in HSCs

Submitted 23 January 2019; accepted 26 May 2019. DOI 10.1182/bloodadvances.2019032169.

The full-text version of this article contains a data supplement.

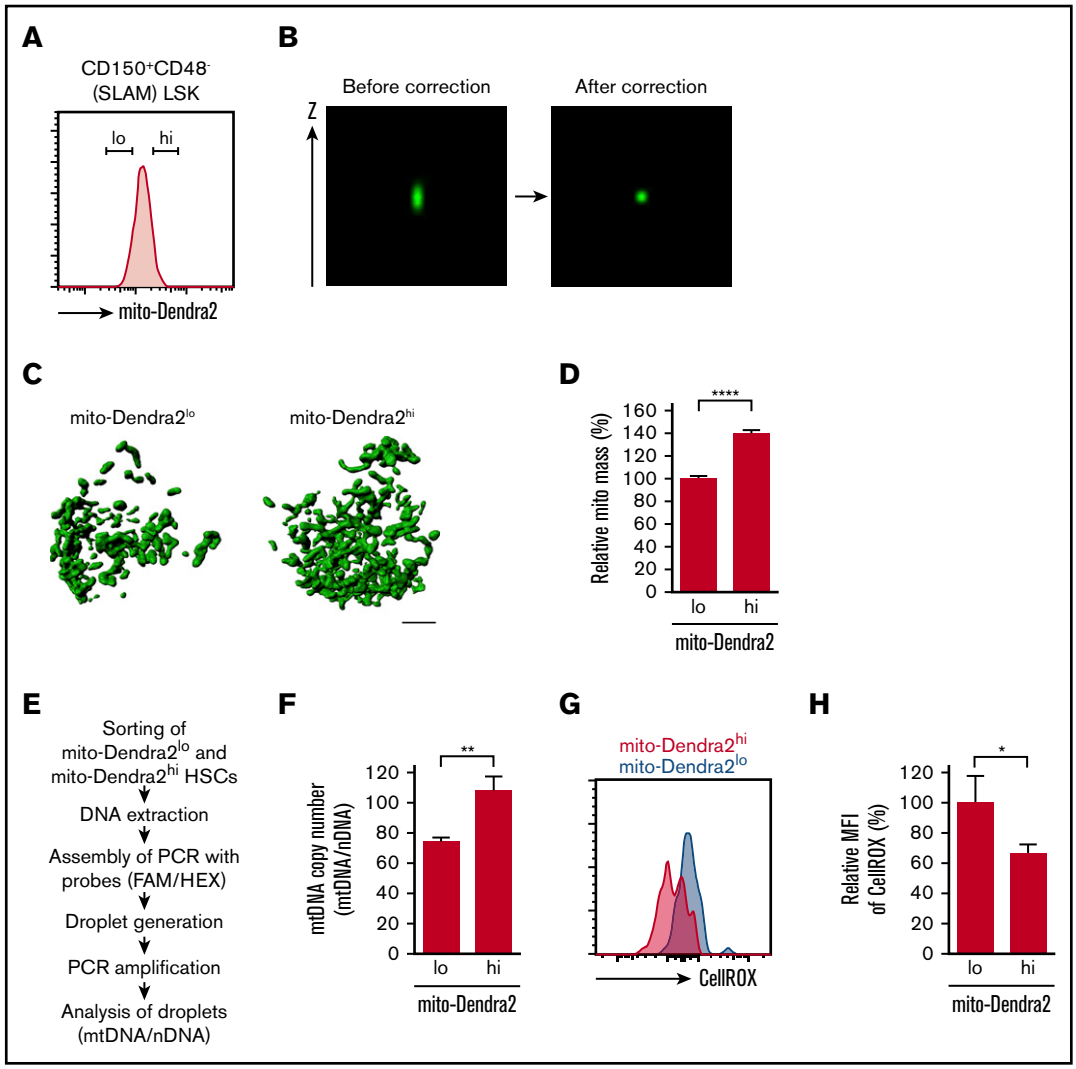

Figure 1. mito-Dendra2^{hi} HSCs have higher mitochondrial mass than mito-Dendra2^{lo} HSCs. (A) Representative flow cytometric graph for gating of mito-Dendra2^{lo} (bottom 10%) and mito-Dendra2^{hi} (top 10%) fractions within BM HSCs (SLAM LSK cells) obtained from mito-Dendra2 mice. (B) Representative superresolution images of fluorescent microspheres (diameter, 0.18 μm) before (left panel) and after (right panel) PSF correction. (C) Representative isosurface rendering of PSF-corrected super-resolution images of mito-Dendra2^{lo} (left panel) and mito-Dendra2^{hi} (right panel) HSCs. Scale bar, 2 μm. (D) Mitochondrial mass in mito-Dendra2^{lo} and mito-Dendra2^{hi} HSCs determined by superresolution images with PSF correction (mean ± standard error of the mean [SEM]; n > 60 each). (E) Schematic flow showing the absolute quantification of mitochondrial DNA copy number (mtDNA/nDNA) using ddPCR. (F) Mitochondrial DNA copy number in mito-Dendra2^{lo} and mito-Dendra2^{hi} HSCs determined by ddPCR (mean ± SEM; n = 7 each). (G) Representative flow cytometric graph of CellROX fluorescence intensity in mito-Dendra2^{lo} and mito-Dendra2^{hi} HSCs. (H) Cellular ROS levels in mito-Dendra2^{lo} and mito-Dendra2^{hi} HSCs (mean ± standard deviation [SD]; n = 3 each). *$P < .05$, **$P < .01$, ****$P < .0001$, Student *t* test.

(Figure 1C). Notably, we observed higher mitochondrial mass in mito-Dendra2^{hi} HSCs compared with mito-Dendra2^{lo} HSCs (Figure 1C-D). To confirm this observation, we used ddPCR for absolute quantification of mitochondrial DNA copy number (Figure 1E) and found that mito-Dendra2^{hi} HSCs had higher mitochondrial DNA copy number than mito-Dendra2^{lo} HSCs (Figure 1F). These results indicate that mitochondrial mass varies among HSCs and confirm that mito-Dendra2^{hi} HSCs have higher mitochondrial mass than mito-Dendra2^{lo} HSCs.

In addition, the expression levels of electron transport chain–related genes were lower in mito-Dendra2^{hi} HSCs (supplemental Figure 1B), whereas the expression of glycolysis-related, mitochondrial fission–related, and mitochondrial fusion–related genes was comparable between mito-Dendra2^{lo} and mito-Dendra2^{hi} HSCs (supplemental Figures 1C and 2A). Consistent with the lower expression of electron transport chain–related genes, mito-Dendra2^{hi} HSCs also displayed lower intracellular ROS levels than mito-Dendra2^{lo} HSCs (Figure 1G-H), thereby suggesting that electron transport chain activity is lower in mito-Dendra2^{hi} HSCs.

To further characterize the mito-Dendra2^{hi} HSC fraction, we compared the expression of HSC-related genes between mito-Dendra2^{lo} and mito-Dendra2^{hi} HSCs (Figure 2A; supplemental Figure 3A). Interestingly, mito-Dendra2^{hi} HSCs expressed significantly lower levels of *Cd34* and higher levels of *Procr* (encodes

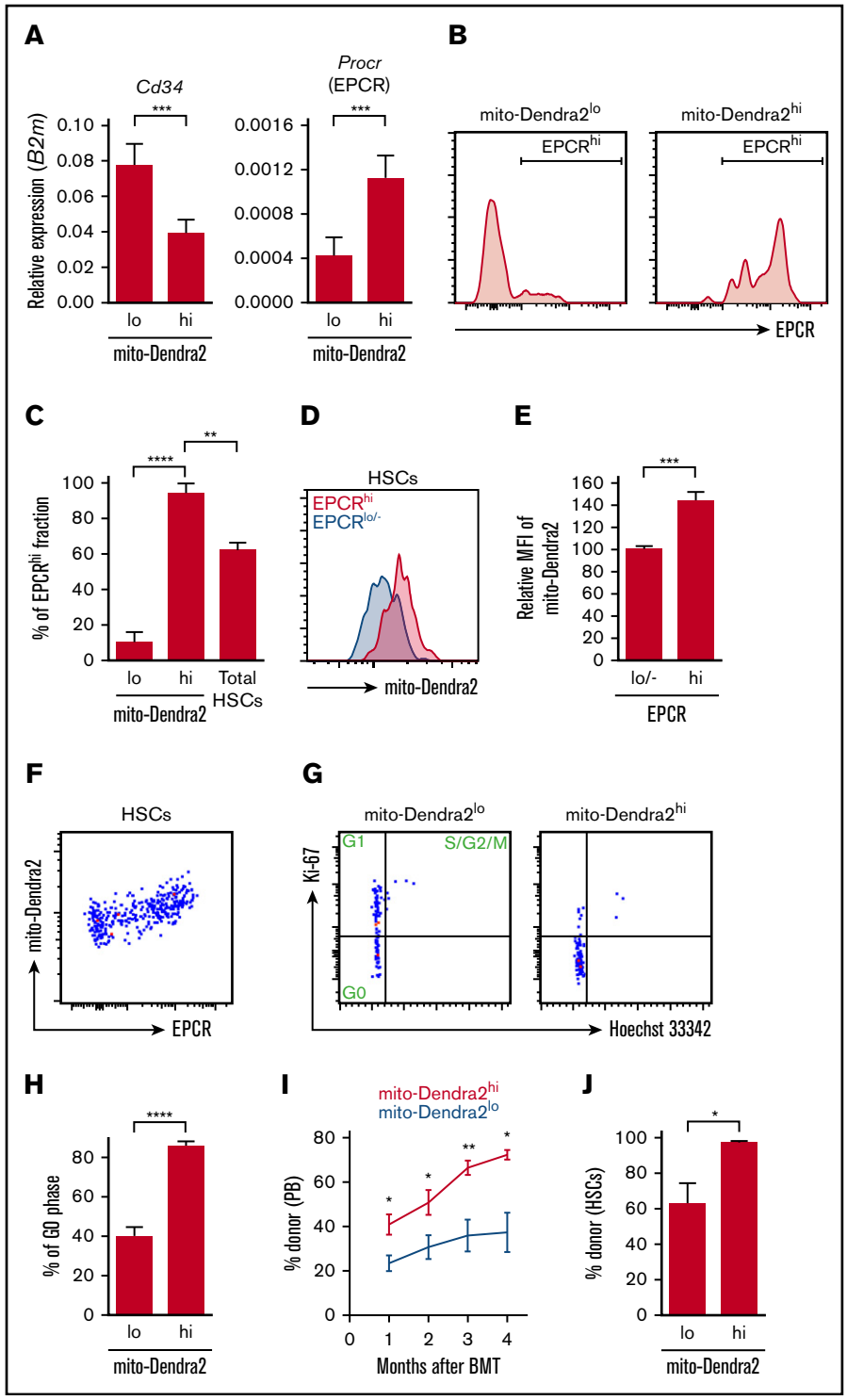

Figure 2. mito-Dendra2^{hi} HSCs are more quiescent and have greater reconstitution capacity than mito-Dendra2^{lo} HSCs. (A) Relative expression of *Cd34* and *Procr* (EPCR) normalized to *B2m* expression in mito-Dendra2^{lo} and mito-Dendra2^{hi} HSCs quantified by reverse transcription polymerase chain reaction (mean ± SD; n = 5 each). (B) Representative flow cytometric graphs of EPCR expression in mito-Dendra2^{lo} (left panel) and mito-Dendra2^{hi} (right panel) HSCs. (C) Frequency of EPCR^{hi} HSCs within mito-Dendra2^{lo}, mito-Dendra2^{hi}, and total HSC fractions (mean ± SD; n = 3 each). (D) Representative flow cytometric graph of mito-Dendra2 fluorescence intensity in EPCR$^{lo/-}$ and EPCR^{hi} HSCs. (E) Median fluorescence intensity of mito-Dendra2 in EPCR$^{lo/-}$ and EPCR^{hi} HSCs (mean ± SD; n = 3 each). (F) Representative flow cytometric plots showing the correlation between mito-Dendra2 fluorescence intensity and EPCR expression of HSCs. (G) Representative flow cytometric plots showing cell cycle profiles of mito-Dendra2^{lo} and mito-Dendra2^{hi} HSCs. (H) Frequency of G0 phase cells within mito-Dendra2^{lo} and mito-Dendra2^{hi} HSCs (mean ± SD; n = 4 each). (I) Monthly peripheral blood (PB) chimerism of mononuclear cells in Ly5.1 recipients transplanted with mito-Dendra2^{lo} or mito-Dendra2^{hi} ESLAM LSK cells (250 cells) and Ly5.1 competitor cells (2×10^5 cells) over 4 months posttransplantation (mean ± SEM; n = 4 or 5 each). (J) BM chimerism of HSCs in the Ly5.1 recipients transplanted with mito-Dendra2^{lo} or mito-Dendra2^{hi} ESLAM LSK cells 4 months posttransplantation (mean ± SEM; n = 4 or 5 each). *$P < .05$, **$P < .01$, ***$P < .001$, ****$P < .0001$, Student *t* test.

EPCR) compared with mito-Dendra2^{lo} HSCs. Because EPCR expression has been reported to strongly correlate with HSC function,[12] we next compared the expression of EPCR between mito-Dendra2^{lo} and mito-Dendra2^{hi} HSCs. The frequency of EPCR^{hi} HSCs was higher within the mito-Dendra2^{hi} HSC fraction than within the mito-Dendra2^{lo} HSC fraction (Figure 2B-C). In addition, the frequency of EPCR^{hi} HSCs within the mito-Dendra2^{hi} HSC fraction was significantly higher than the frequency of EPCR^{hi} HSCs in the total HSC population (Figure 2C). We also compared the mito-Dendra2 fluorescence intensity between EPCR$^{lo/-}$ and EPCR^{hi} HSCs; importantly, the median fluorescence intensity was higher in EPCR^{hi} HSCs (Figure 2D-E). When mito-Dendra2 fluorescence intensity was plotted against EPCR expression, it correlated positively with EPCR expression in HSCs (Figure 2F),

thus suggesting that mito-Dendra2^{hi} HSCs contain HSCs with greater HSC potential.

We next studied the association between mitochondrial mass and cell cycle state and observed that mito-Dendra2^{hi} HSCs exhibited a higher frequency of quiescent (G0) cells than did mito-Dendra2^{lo} HSCs (Figure 2G-H). Correspondingly, mito-Dendra2^{hi} HSCs had lower expression of the cell cycle–associated genes *Myc* and *Cdk6*, but higher expression of the negative cell cycle regulator *Cdkn1c*, compared with mito-Dendra2^{lo} HSCs (supplemental Figure 3B). Under stress hematopoiesis induced by 5-fluorouracil (5-FU) injection, the number of Lin$^-$EPCR^{hi}CD150$^+$CD48$^-$ HSCs[9] decreased 2 days after 5-FU injection and recovered 7 days after 5-FU injection (supplemental Figure 4A). On the other hand, the number of mito-Dendra2^{hi} Lin$^-$EPCR^{hi}CD150$^+$CD48$^-$ HSCs remained low 7 days after 5-FU injection (supplemental Figure 4B), which is consistent with cell cycle entry and proliferation of most HSCs 7 days after 5-FU injection.[9] Therefore, these observations suggest that mito-Dendra2^{hi} HSCs are more quiescent than mito-Dendra2^{lo} HSCs.

To determine whether mitochondrial mass is associated with reconstitution capacity in HSCs, we conducted competitive BM transplantation of mito-Dendra2^{lo} or mito-Dendra2^{hi} HSCs with Ly5.1 competitor cells into lethally irradiated Ly5.1 recipients. Recipients transplanted with mito-Dendra2^{hi} HSCs exhibited significantly higher chimerism of PB mononuclear cells (MNCs) (supplemental Figure 5A-B) and BM HSCs (supplemental Figure 5C-D) compared with recipients transplanted with mito-Dendra2^{lo} HSCs. Secondary BM transplantation also revealed higher PB MNC and BM HSC chimerism in mice transplanted with mito-Dendra2^{hi} HSCs (supplemental Figure 5E-F), suggesting that long-term HSCs are enriched in the mito-Dendra2^{hi} HSC fraction. No difference in homing capacity was observed between mito-Dendra2^{lo} and mito-Dendra2^{hi} LSK cells (supplemental Figure 6A). Using additional gating of EPCR, we observed that recipients transplanted with mito-Dendra2^{hi} EPCR^{hi}CD150$^+$CD48$^-$ (ESLAM)[16] LSK cells exhibited higher PB MNC chimerism than recipients transplanted with mito-Dendra2^{lo} ESLAM LSK cells over 4 months posttransplantation, whereas PB chimerism in recipients with mito-Dendra2^{lo} ESLAM LSK cells progressively increased (Figure 2I). Moreover, analysis of HSC chimerism in BM 4 months posttransplantation showed higher chimerism in recipients transplanted with mito-Dendra2^{hi} ESLAM LSK cells compared with those transplanted with mito-Dendra2^{lo} ESLAM LSK cells which also exhibited significant chimerism of HSCs (Figure 2J). Taken together, these results indicate that mito-Dendra2^{hi} HSCs have a greater reconstitution capacity than mito-Dendra2^{lo} HSCs.

In this study, we identified a significant variation in mitochondrial mass among HSCs. HSCs with higher mitochondrial mass were more quiescent and exhibited greater reconstitution capacity. Thus, high mito-Dendra2 fluorescence intensity enriches quiescent and potent HSCs. Because mitochondrial membrane potential has been reported to be low in quiescent HSCs,[9] our study may suggest a mass/function paradox regarding mitochondria in HSCs. The quality and function of mitochondria in quiescent HSCs should be clarified in the future.

Acknowledgments

The authors thank Yang Chong, Jessica L. Berlier, Michelle Meng Huang Mok, Tamie Endoh, A'Qilah Banu Binte Abdul Majeed, Muddineni Siva Sai Naga Anurag, Nur Humaira Binte Fua'Di, Samuel Ko, Aled O'Neill, Malini Rethnam, and Shu Ying Lee for advice, help, and discussions regarding experiments.

This work was supported by the National Research Foundation of Singapore and the Singapore Ministry of Education under its Research Centres of Excellence initiative, the Singapore Ministry of Health's National Medical Research Council (NMRC) Singapore Translational Research (STaR) Investigator Award (NMRC/STaR/0019/2014) (T.S.) and Clinician Scientist–Individual Research Grant–New Investigator Grant (NMRC/CNIG/1181/2018) (Y.T.), the Uehara Memorial Foundation Overseas Research Fellowship (Y.T.), and the Japan Ministry of Education, Culture, Sports, Science and Technology (MEXT) KAKEN Grant-in-Aid for Scientific Research (S) (26221309) (T.S.).

Authorship

Contribution: Y.T. and A.N.-I. designed the study and wrote the first draft of manuscript; D.Q.T. and M.F. revised the manuscript; and all authors analyzed and interpreted the results and read and approved the final version of the manuscript.

Conflict-of-interest disclosure: The authors declare no competing financial interests.

ORCID profiles: D.Q.T., 0000-0001-8303-9100; M.F., 0000-0003-4868-0677; M.H., 0000-0003-1673-3340.

Correspondence: Toshio Suda, Cancer Science Institute of Singapore, Centre for Translational Medicine, National University of Singapore, 14 Medical Dr, #12-01, Singapore 117599, Singapore; e-mail: csits@nus.edu.sg.

References

1. Nakamura-Ishizu A, Takizawa H, Suda T. The analysis, roles and regulation of quiescence in hematopoietic stem cells. *Development*. 2014;141(24):4656-4666.
2. Wilson A, Laurenti E, Oser G, et al. Hematopoietic stem cells reversibly switch from dormancy to self-renewal during homeostasis and repair. *Cell*. 2008;135(6):1118-1129.
3. Simsek T, Kocabas F, Zheng J, et al. The distinct metabolic profile of hematopoietic stem cells reflects their location in a hypoxic niche. *Cell Stem Cell*. 2010;7(3):380-390.
4. Takubo K, Nagamatsu G, Kobayashi CI, et al. Regulation of glycolysis by Pdk functions as a metabolic checkpoint for cell cycle quiescence in hematopoietic stem cells. *Cell Stem Cell*. 2013;12(1):49-61.
5. Ito K, Suda T. Metabolic requirements for the maintenance of self-renewing stem cells. *Nat Rev Mol Cell Biol*. 2014;15(4):243-256.
6. Suda T, Takubo K, Semenza GL. Metabolic regulation of hematopoietic stem cells in the hypoxic niche. *Cell Stem Cell*. 2011;9(4):298-310.

7. Tan DQ, Suda T. Reactive oxygen species and mitochondrial homeostasis as regulators of stem cell fate and function. *Antioxid Redox Signal*. 2018; 29(2):149-168.

8. Luchsinger LL, de Almeida MJ, Corrigan DJ, Mumau M, Snoeck HW. Mitofusin 2 maintains haematopoietic stem cells with extensive lymphoid potential. *Nature*. 2016;529(7587):528-531.

9. Umemoto T, Hashimoto M, Matsumura T, Nakamura-Ishizu A, Suda T. Ca^{2+}-mitochondria axis drives cell division in hematopoietic stem cells. *J Exp Med*. 2018;215(8):2097-2113.

10. de Almeida MJ, Luchsinger LL, Corrigan DJ, Williams LJ, Snoeck HW. Dye-independent methods reveal elevated mitochondrial mass in hematopoietic stem cells. *Cell Stem Cell*. 2017;21(6):725-729.e4.

11. Pham AH, McCaffery JM, Chan DC. Mouse lines with photo-activatable mitochondria to study mitochondrial dynamics. *Genesis*. 2012;50(11):833-843.

12. Balazs AB, Fabian AJ, Esmon CT, Mulligan RC. Endothelial protein C receptor (CD201) explicitly identifies hematopoietic stem cells in murine bone marrow. *Blood*. 2006;107(6):2317-2321.

13. Gur-Cohen S, Itkin T, Chakrabarty S, et al. PAR1 signaling regulates the retention and recruitment of EPCR-expressing bone marrow hematopoietic stem cells [published correction appears in *Nat Med*. 2016;22(4):446]. *Nat Med*. 2015;21(11):1307-1317.

14. Kiel MJ, Yilmaz OH, Iwashita T, Yilmaz OH, Terhorst C, Morrison SJ. SLAM family receptors distinguish hematopoietic stem and progenitor cells and reveal endothelial niches for stem cells. *Cell*. 2005;121(7):1109-1121.

15. Bonora M, Ito K, Morganti C, Pinton P, Ito K. Membrane-potential compensation reveals mitochondrial volume expansion during HSC commitment. *Exp Hematol*. 2018;68:30-37.e1.

16. Wilson NK, Kent DG, Buettner F, et al. Combined single-cell functional and gene expression analysis resolves heterogeneity within stem cell populations. *Cell Stem Cell*. 2015;16(6):712-724.